We are IntechOpen, the world's leading publisher of Open Access books Built by scientists, for scientists

6,900
Open access books available

185,000
International authors and editors

200M
Downloads

Our authors are among the

154
Countries delivered to

TOP 1%
most cited scientists

12.2%
Contributors from top 500 universities



WEB OF SCIENCE™

Selection of our books indexed in the Book Citation Index in Web of Science™ Core Collection (BKCI)

Interested in publishing with us?
Contact book.department@intechopen.com

Numbers displayed above are based on latest data collected.
For more information visit www.intechopen.com



5

Method to Indentify Nonsignificant Responses at Multifocal Electroretinogram Recordings: Technical Note

Aline Corrêa de Carvalho[1], Givago da Silva Souza[1,2], Bruno Duarte Gomes[2], Anderson Raiol Rodrigues[1], Dora Fix Ventura[3] and Luiz Carlos de Lima Silveira[1,2]
[1]*Universidade Federal do Pará, Núcleo de Medicina Tropical*
[2]*Universidade Federal do Pará, Instituto de Ciências Biológicas*
[3]*Universidade de São Paulo, Instituto de Psicologia*
Brazil

1. Introduction

Multifocal electroretinography (mfERG) was developed by Erich Sutter and colleagues (Sutter & Tran, 1992) and since the beginning was an important non invasive method to record simultaneously evoked electrical activity from several retinal areas in a relative short time. This method may reveal the presence or absence of electrical activity in a number of retinal locations, mapping the functional state of a large retinal area.

The stimulus is composed by multiple patches. Usually, each patch has a command to show flashes according to a pseudorandom sequence called binary m-sequence. The decision to show or not a flash in the patch is programmed in periodic intervals, the base period (Sutter, 2000). The evoked responses, called kernels, are derived from a cross-correlation technique (Sutter, 2001).

Usually, the stimulus is scaled in order to elicit similar waveforms across the visual field. The results of an mfERG session is presented in an array of traces or in a three dimensional plot showing the response density to the different sectors of the stimulus. The response density plot may lead the clinician to misinterpretation, because the plot generates a central peak, even when no responses are recorded from the patient (Kretschmann et al., 2000; Hood et al., 2003). Waveform array is safer than response density to decide about an outcome of the mfERG test. It is relatively easy for clinicians to recognize true responses (large signal plus noise) in the mfERG trace array. However, it is very difficult to decide between decreased responses (small signal plus noise), and pure noise.

Some analysis methods have suggested different ways to discriminate signal from noise in recorded data that can be applied to a variety of electrophysiological techniques. It was shown that the dot product between the responses and an artificial signal template could increase the signal-to-noise ratio (SNR) of the data (Sutter & Tran, 1992). Few studies have suggested objective methods to evaluate the reliability of the mfERG (Hood et al., 1998, Seeliger et al., 1998). Hood et al. (1998) proposed the comparison of the signal RMS

amplitude of the recording with the RMS amplitude of a template in different time intervals. The closer in time was the equivalence between both RMS amplitudes, the better was the SNR. Seeliger et al. (1998) measured mfERG implicit times to determine their distribution across the retina. They found a low intersubject variability and higher implicit times in the blind spot, upper and lower retina, and macula. They calculated the median of implicit time of each sector of normal subjects and subtracted this value from the implicit times of patients. The larger the difference, the higher the chance to find a functionally decreased area. Other work compared human scores and automated methods to distinguish signal information of mfERG from noise. The authors concluded that automated routines can be used to increase the sensitivity of signal detection of the mfERG compared to human scoring (Wright et al., 2006).

Here, we describe a method to identify an optimal SNR that can be used to classify waveforms with normal amplitude, low amplitude and without signal.

2. Subjects

We recorded mfERGs from 10 healthy subjects (25.4 ± 3.5 years old). Their pupils were dilated and their eyes were anesthetised before electrode placement (Mydriatics. Tropicamide 1%, Alcon; Phenylephrine chloridrate 10%, Allergan. Anesthetic. Proximetacaine chloridrate 0.5%, Alcon). All procedures were in agreement with the tenets of the Declaration of Helsinki and approved by the Research Ethics Committee of the Tropical Medicine Nucleus, Federal University of Pará, Report 57/2008 of 26th November 2008, following the Resolution 196/96 of the National Health Council of Brazil.

3. Visual stimulation

VERIS Science v6.0.5d (Electro-Diagnostic Imaging, EDI, San Mateo, California) was used to generate a black-and-white stimulus comprising a 103 hexagons array covering 45° x 45° of visual field. The stimulus was generated in a colour microdisplay (FMS II, EDI) at 60 Hz frame rate and 1280 x 1024 pixels of spatial resolution. The microdisplay was positioned in front of subject's eye and the optical distance from the eye to the stimulus was adjusted until the best focus was achieved.

The hexagons were scaled with eccentricity to equalize response amplitude across the visual field following ISCEV recommendations (Hood et al., 2008). The luminance of each hexagon was modulated in time by a complete cycle of an m-sequence of 2^{14} -1 elements (Sutter & Tran, 1992). The same m-sequence was used for all hexagons but its starting point was displaced in time from one hexagon to the other. States 1 and -1 of the m-sequence represented the flash and non flash period, respectively. The base period was 16.667 ms (the duration of 1 frame). The stimulation session lasted 4 min and 33 s divided in eight segments of 34.13 s each. A red cross of 1° of visual angle was used as fixation mark. The eye fixation was continuously monitored during visual stimulation by an infrared camera located inside the microdisplay.

4. Recordings

Continuous recordings were obtained by using a Burian-Allen corneal electrode, housing both the recording and reference electrodes, and a ground consisting of a gold-cup surface

electrode placed on the subject's ear lobe. Electrode impedance was monitored between stimulus segments and kept below 2 kΩ. The bioelectrical signals were x 50,000 amplified, sampled at 16 times per frame (about 960 Hz), and on-line band-filtered at 10-300 Hz using a 15LT differential amplifier (Grass, Quincy, Massachusetts). An acquisition board (PCI ESeries, National Instruments, Austin, Texas) was used to digitize the analog signal.

5. Description of the method

5.1 RMS amplitude ratio calculus

The VERIS Science v6.0.5d (EDI) software was used to extract the first order kernel. The first order kernel waveform data for the 0-200 ms interval was exported to be analysed by a homemade routine written for MATLAB environment (The Mathworks, Natick, Massachusetts).

We calculated a RMS amplitude ratio for each local mfERG response for all subjects (Zhang et al., 2002). First, we calculated the RMS amplitude of the first order kernel for the signal time interval, located between 0-80 ms, and the RMS amplitude for a time interval comprising only noise uncorrelated with visual stimulation, located between 120-200 ms (Equations 1 and 2, respectively) (Figure 1 shows the noise and signal time intervals for an mfERG recording).

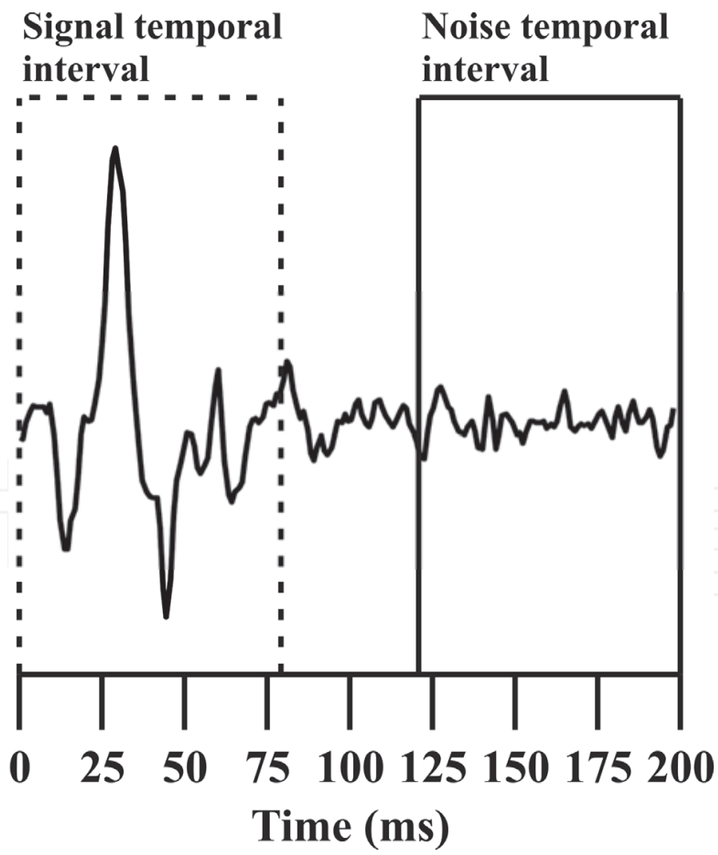


Fig. 1. mfERG waveform. The RMS amplitude of the signal time interval and noise time interval were calculated for all 103 waveforms to quantify a RMS amplitude ratio associated to the signal and noise information of each waveform.

Then, we estimated the ratio between the signal RMS amplitude of the jth hexagon to the mean noise RMS amplitude of the 103 mfERG waveforms obtained from the same subject (Signal Ratio, Equation 3). To obtain an equivalent value for the noise interval, we divided the noise RMS amplitude of the jth hexagon by the mean noise RMS amplitude (Noise Ratio, Equation 4).

$$\text{Signal amplitude} = \sqrt{\frac{\sum_{t=0}^{80} (Rt - \mu_{0 \text{ to } 80})^2}{N}} \quad (1)$$

Signal amplitude of a waveform is the RMS amplitude calculated over the signal time interval of the jth hexagon recording, Rt is the absolute amplitude at time t, μ0 to 80 is the mean amplitude during the signal time interval, and N is number of samples in the signal time interval.

$$\text{Noise amplitude} = \sqrt{\frac{\sum_{t=120}^{200} (Rt - \mu_{120 \text{ to } 200})^2}{N}} \quad (2)$$

Noise amplitude of a waveform is the RMS amplitude calculated over the noise time interval of the jth hexagon recording, Rt is the absolute amplitude at time t, μ0 to 200 is the mean amplitude during the noise time interval.

$$\text{Signal ratio} = \frac{\text{Signal amplitude}}{\text{Mean Noise amplitude}_{\text{hexagon (1 to 103)}}} - 1 \quad (3)$$

Signal Ratio of a waveform is the signal to noise ratio (SNR) to the signal time interval for the jth hexagon recording. Mean Noise amplitude is the average of the noise RMS amplitude for the 103 hexagon waveforms for the same subject.

$$\text{Noise ratio} = \frac{\text{Noise amplitude}}{\text{Mean Noise amplitude}_{\text{hexagon (1 to 103)}}} - 1 \quad (4)$$

Noise Ratio of a waveform is the equivalent to the SNR to the noise time interval for the jth hexagon recording.

5.2 Looking for an optimal RMS amplitude ratio to discriminate normal waveforms from waveforms without signal

For this first analysis, our data were composed of 1030 signal ratios and 1030 noise ratios. We estimated the distribution of frequency of RMS amplitude ratio (Signal ratio and Noise ratio). We then estimated the associated cumulative distribution function for the noise and the signal data distribution (Figure 2A-B). We proceeded to perform a Receiver Operating Characteristic (ROC) analysis using as false positive rate the values of 1 - noise cumulative distribution function and using the signal cumulative distribution function as true positive rate (Figure 2C-D). We obtained the optimal RMS amplitude ratio to distinguish the signal data from noise data as being the one which corresponds to a higher associated trade-off in the ROC space. The trade-off was calculated as the difference between each pair of true positive rate and false positive rate in the ROC space (Figure 2C-D). The optimal RMS amplitude ratio was 0.47.

5.3 Looking for an optimal RMS amplitude ratio to discriminate normal waveforms from waveforms with attenuated signal

In the previous section, we calculated an optimal RMS amplitude ratio to distinguish normal waveforms from those with no signal. But in clinical research we need to know how to distinguish the normal response from responses with different levels of decreased signal amplitude. In order to find an optimal RMS amplitude ratio for this purpose, we first artificially attenuated the original waveforms in a way that the signal could be decreased while keeping the noise level constant. This attenuation method was described by Wright et al. (2006).

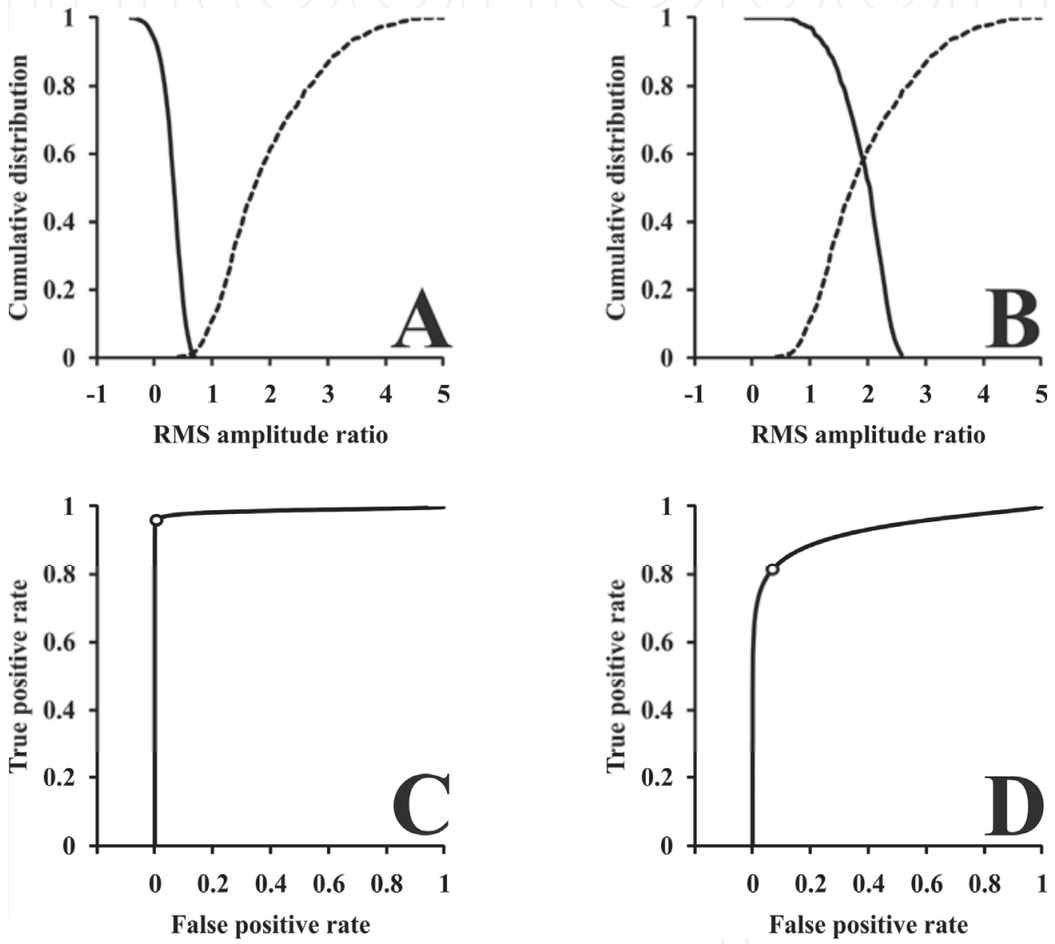


Fig. 2. Analysis implemented to obtain optimal values to distinguish between original waveforms and attenuated waveforms. (A) Cumulative distribution functions (CDF) of noise information (continuous line) and original signal information (dotted line). (B) CDF of attenuated signal information at level 1 (continuous lines) and signal information (dotted line). (C) ROC analysis correlating the CDF from signal and CDF from noise. (D) ROC analysis correlating attenuated signal at level 1 and original signal. The circles at the ROC curves, in C and D, are the higher trade-off between true positive rate and false positive rate. The RMS amplitude ratios associated to the higher trade-off in the ROC space were considered as the optimal values to distinguish two data groups. Functions using data of other attenuation levels are intermediate between the functions showed in this figure.

To attenuate the amplitude of the signal from each waveform, the noise data was added to the signal. The attenuation level corresponded to the number of times the noise data was added to the signal (number of summations between signal and noise). The result was then divided by the attenuation level plus one to keep constant the RMS amplitude of the noise (Equation 5).

$$\text{jth AttenuateWave} = \frac{\text{jth Wave}_{0 \text{ to } 80} + (\text{attenuation level} \times \text{jth Wave}_{120 \text{ to } 200})}{\text{attenuation level} + 1} \quad (5)$$

The jth AttenuateWave 0 to 80 is the attenuated signal time interval data, jth Wave 0 to 80 is the original signal time interval data, attenuation level is the number of times that the noise data will be added to the signal data, and the jth Wave120 to 200 is the noise time interval data.

We used 5 attenuation levels, from 1 to 5, in order to simulate different visual loss conditions. Figure 3 shows a scheme representing the different artificial attenuation levels over the same signal in an original waveform.

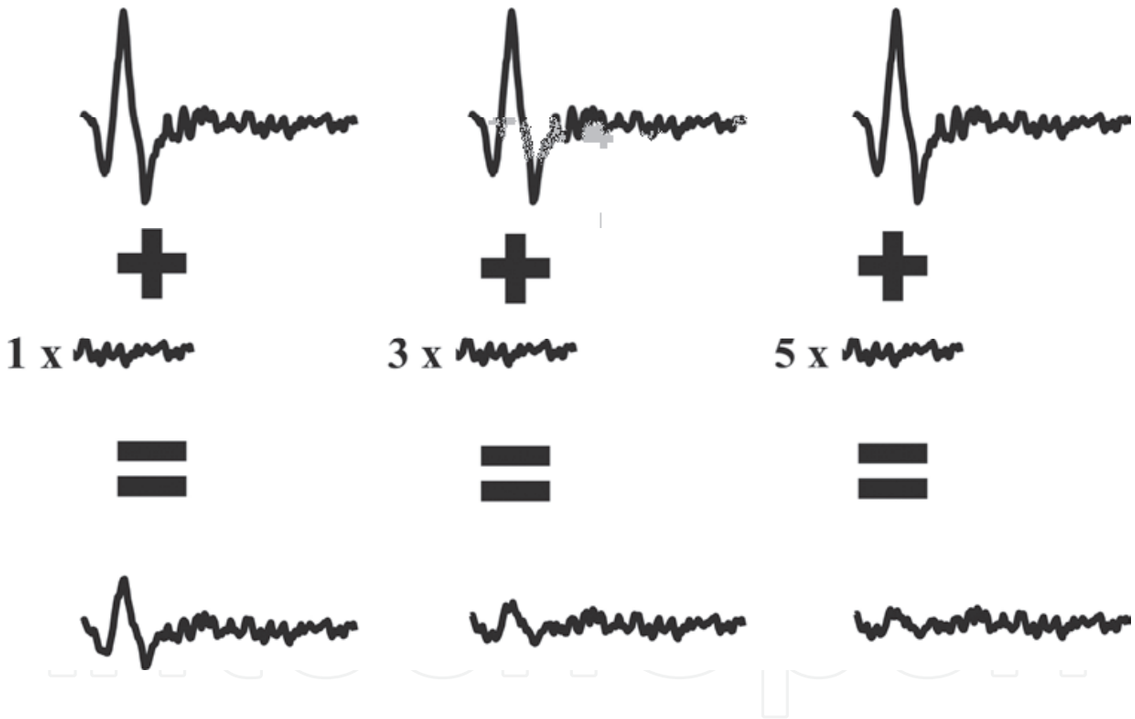


Fig. 3. Diagram representing the artificial attenuation applied over the signal from original waveforms. From left to right, the attenuation level is increasing. Consequently, the signal of the waveform is decreasing. Noise level was kept constant (similar RMS amplitude) across the attenuation levels because the denominator of equation 5 used to normalise the waveforms was dependent how much noise was added in the signal.

Then, the procedure of the previous section was repeated, but now we replaced the noise information by the attenuated signal information. The optimal values found to distinguish the original signal information from attenuated waveforms are indicated in the Table 1.

5.4 Testing the reliability of the optimal RMS amplitude ratios to different waveform attenuation conditions

We quantified the amount of errors that a classifier can present when using each optimal RMS amplitude ratio to distinguish normal waveforms from noisy or attenuated waveforms in different levels. The role of the classifier was to compare the signal ratio of waveforms to each optimal value obtained previously for the different attenuation levels.

Attenuation level	Optimal value
Noise	0.47
5	0.44
4	0.48
3	0.57
2	0.78
1	1.21

Table 1. Optimal value of differentiation from signal waveforms to attenuated waveforms. The optimal value was the RMS amplitude ratio with highest trade-off between hit and errors.

Before the attenuation process, the classifier considered that all waveforms should have signal ratio above the optimal SNR to distinguish normal from any attenuated waveform. We considered as error of classification when after the attenuation process the attenuated signal RMS amplitude ratio was higher than the optimal value. Correct identification was considered when the signal ratio of a waveform was lower than the optimal value.
The hit rate (HR) of the automated classifier was calculated by Equation 6. Table 2 shows the HR obtained by the classifier using each optimal RMS amplitude ratio to distinguish normal waveforms from the different attenuation levels.

$$HR = \frac{\text{correct responses}}{(\text{correct responses} + \text{errors})} \quad (6)$$

The best performance of the classifier in identifying highly attenuated waveforms (attenuation levels 4 and 5) occurred when the optimal value was 0.57. For moderately attenuated waveforms (attenuation levels 2 and 3) the best performance occurred when the optimal value was 0.78, and for slightly attenuated waveforms (attenuation level 1) it occurred with an optimal value of 1.21.
Our analysis seemed to be able to delimit a range of RMS amplitude ratios to classify any mfERG waveform obtained from 103 hexagons array (Table 3). It can be argued if the attenuated waveforms at the level 1 already correspond to a true visual loss or is within the variability of an electrophysiological amplitude recording, but the moderately and highly attenuated waveforms have a considerable decrease of the signal amplitude and their clinical importance must be considered.
For an application to a real situation, we applied the evaluation protocol to recordings obtained from a patient affected by ocular toxoplasmosis. Figure 4 shows the mfERG array of this patient after the analysis, showing the retinal waveforms associated with the retinal scar marked in different colours to indicate Table 3.
We think the same method could be applied for sets of waveforms obtained from other hexagons arrays, in order to find the optimal ranges to classify mfERG waveforms.

Hit rate (%)					
Optimal value	A.L. 5	A.L. 4	A.L. 3	A.L. 2	A.L. 1
0.47	99 ± 0.8	98.9 ± 0.9	96.4 ± 3.5	84.7 ± 16.7	51.5 ± 30.7
0.44	98.4 ± 1.7	97.5 ± 3.1	94 ± 7.1	81.1 ± 21.3	46.5 ± 32.5
0.48	98.7 ± 1.5	98.3 ± 2.3	95.3 ± 5.8	83.6 ± 18.7	50.4 ± 33
0.57	**99.3 ± 0.7**	**99 ± 1.2**	97.1 ± 4.6	88.6 ± 14.5	57.1 ± 35
0.78	97.6 ± 3	97.6 ± 3	**97.4 ± 2.9**	**94.2 ± 6.1**	68.7 ± 30.4
1.21	81.7 ± 19.3	81.7 ± 19.3	81.7 ± 19.3	81.7 ± 19.2	**73.4 ± 15**

Table 2. Hit rate estimated for the usage of the optimal values in different attenuation levels. The classifier had a better performance in distinguishing normal waveforms from slightly attenuated waveforms (A.L. 1) using the optimal value 1.21, whilst the optimal value of 0.78 was better to differentiate normal waveforms from those with intermediate attenuation (A.L. 2 and 3), and the optimal value of 0.57 was better to distinguish highly attenuated or noisy waveforms (AL. 4 and 5) from the original waves. A.L.: Attenuation level.

6. Discussion

Since the development of the mfERG technology in the 90's, it was immediately applied to different topics of clinical ophthalmology (Huang et al., 1996; Kretschmann et al., 1998; Ventura et al., 2004; Greenstein et al., 2004; Raster et al., 2011), and over 700 articles already discussed the technique. The experience of the ophthalmologist is very important in the functional mapping, but this topographical evaluation is still very subjective (Hood et al., 2003). The method that we are suggesting could be an objective alternative to the conventional subjective evaluation of mfERG.

Classification of mfERG waveform	
Highly attenuated amplitude	SNR < 0.57 (Hit rate > 97%-99%)
Moderately attenuated amplitude	0.78 > SNR ≥ 0.57 (Hit rate ≈ 94 - 97%)
Slightly attenuated amplitude	1.21 > SNR ≥ 0.78 (Hit rate ≈ 73%–94%)
Normal waveforms	SNR ≥ 1.21 (Hit rate ≈ 73%)

Table 3. Classification of mfERG waveforms. Ranges of signal to noise ratio to qualify normal or slightly attenuated waveforms in black, moderately attenuated in yellow, and highly attenuated in red in the Figure 4. In the parenthesis the hit rate of a classifier which use each optimal value.

The application of a SNR evaluation as in the present work in the software that performs mfERG recordings (like Veris system - EDI or Retiscan – Roland Consultant) could help the users to avoid some mistakes in the identification of the waveform as normal response, decreased responses or noise. A color-marked trace array as shown in figure 4 would make the task of the clinician easier.

Another application of the results from SNR analysis would be in the programming of response density plots. It is well established that response density plot can generate a false

central peak in conditions of recordings with no signals (Hood et al., 2003, Hood et al., 2008). After the SNR evaluation, it would be possible to identify the patches related to the absence of responses (for the data of the present work, SNR < 0.57), and it would be possible to program the response density plot with this information, setting zero amplitude in the response density of the hexagon with no response. Figure 5 shows a response density plot of the data shown in Figure 4 with and without the SNR evaluation.

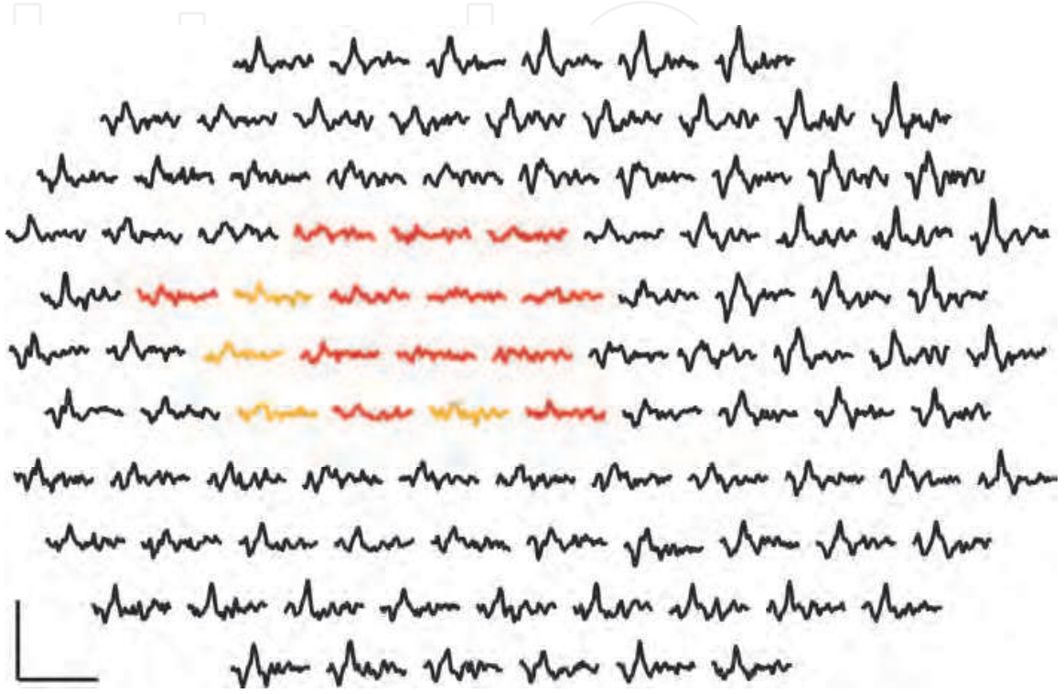


Fig. 4. Evaluation of mfERGs from a patient with visual loss caused by retinal toxoplasmosis. The area of the retinal scar was marked by the protocol in orange (moderately attenuated waveforms) and red (highly attenuated waveforms). Black waveforms indicate normal or slightly attenuated waveforms. Horizontal scale: 100 ms; Vertical scale: 1 μV.

The main contribution of the present technical note is the description of a method to estimate ranges of SNR in order to classify an unknown mfERG waveform. Other methods proposed to measure the difference between mfERG waveform and a template waveform estimated from a control group (Hood & Li, 1997; Wright et al., 2008). The larger the difference between both waveforms, the lower the likelihood that the waveform contained a signal. Seeliger et al. (1998) suggested differences in the implicit time of the P1 component between templates and unknown waveforms. They found high implicit time deviations in recordings obtained from retinitis pigmentosa patients.

The absolute values of SNR can be different when we compare different data settings due different procedures. All data used here was obtained from recordings using Burian-Allen electrodes and 103 hexagons in the stimulus. Other recording and stimulation parameters could change the absolute values of the limit ranges. Other work has described the influence of different experimental conditions in mfERG SNRs (Kretschmann et al., 2000).

The application of our method helps the clinicians to map retinal function and quantify the number of waveforms in each SNR range. It can be of further use as a tool to obtain

parameters of the sequential evaluation of the history of the retinal disease. For the application of our protocol we advise that each laboratory applies it to their own data to obtain the optimal ranges of classification.
In order to facilitate the application of this method by other researchers, in the next section we present the code in MATLAB language of important steps of the method described in the present chapter.

7. Matlab codes for important steps to reproduce the method described in the present technical note

Matlab is a very useful technical programming interpreted language to work with matrix computations. This computational environment has many pre-programmed functions that help a beginner in mathematics or computer science to perform complex numerical calculations in a relative intuitive way. In visual electrophysiology, this language got an important status in the data analysis mainly after multifocal electrophysiology, which requires the researcher to work with multiple vectors simultaneously.

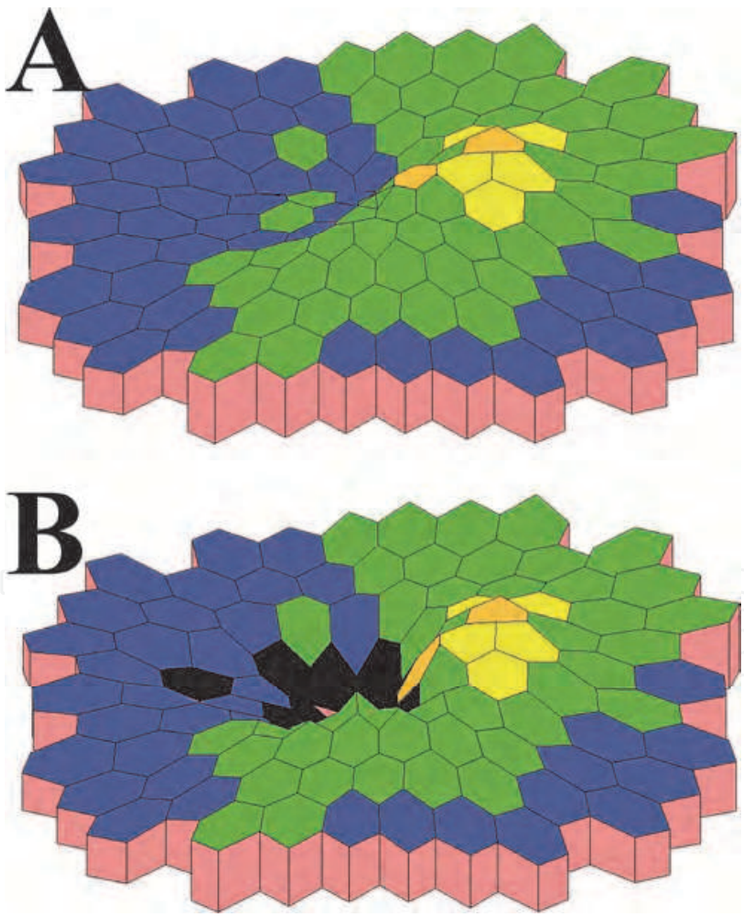


Fig. 5. Response density plots calculated from the same in Figure 4. The plots were programmed without and with SNR evaluation results (A and B, respectively). The hexagons with no responses had zero response density and they are marked in black.

7.1 Code to calculate the Signal ratio and Noise ratio for a subject as described in the equations (3) and (4)

Trace_Array is a matrix with 103 lines and 193 columns. **Trace_Array** represents the waveforms information. Each line represents one of 103 waveforms and each column is each voltage of the recording

```
RMS_Signal = ones(1,103);%RMS_Signal will receive the RMS amplitude of the signal interval
RMS_Noise = ones(1,103);%RMS_Noise will receive the RMS amplitude of the noise interval
SNR_Signal = ones(1,103);%SNR_Signal will receive the Signal ratio
SNR_Noise = ones(1,103);%SNR_Noise will receive the Noise ratio
%Next loop executes the calculus of RMS amplitude of the signal interval
for i = 1:103
   RMS_Signal(1,i) = std(Trace_Array(i,1:78),1);
end
%Next loop executes the calculus of RMS amplitude of the noise interval
for Line= 1:103
   RMS_Noise(1,line) = std(Trace_Array(i,116:193),1);
end
meanRMS_Noise = mean(RMS_Noise);%Calculus of the average of all Noise RMS amplitudes
%Next loop executes the calculus of Signal ratio
for i = 1:103
   SNR_Signal(1,i) = (RMS_Signal(1,i)/meanRMS)-1;
end
%Next loop executes the calculus of Noise ratio
for i = 1:103
   SNR_Noise(1,i) = (RMS_Noise(1,i)/meanRMS_Noise)-1;
end
```

7.2 Code to perform the artificial attenuation in the original waveforms

The code below performs an artificial attenuation in the level 5. To perform other attenuation levels, the user must only change the value of variable **Att_level**

```
Att_Rec = ones(103,193);%Attenuated_recording will receive the attenuated waveforms
Att_level = 5; %Att_level sets the attenuation level to proceed
%Next loop will create build a matrix of attenuated waveforms as indicated in equation (5)
for i = 1:103
Att_Rec(i,:)=[(Trace_Array(i,1:78)+Att_level*Trace_Array(i,116:193))/(F+1),Trace_Array(i,79
:193)];
end
```

7.3 Code to calculate the cumulative distribution of signal information and noise information of the sample

In the next code, **Signal** is the matrix with all Signal ratio values of the sample and **Noise** is the matrix with all Noise ratio values of the sample.

```
interval = 0.05;
max_Signal = max(Signal); % finding maximum value of Signal ratio
min_Noise = min(Noise); %finding minimum value of Noise ratio
x = min_Noise:interval:max_Signal;
data_Signal = histc(Signal,x);%to calculate the number of elements in each Signal ratio of the interval x_Signal
data_Noise = histc(Noise,x); %to calculate the number of elements in each Noise ratio of the interval x_Noise
sum_Signal = sum(data_Signal);
sum_Noise = sum(data_Noise);
percent_sum_Signal = data_Signal ./sum_Signal;
percent_sum_Noise = data_Noise ./sum_Noise;
%Next loop will calculate the cumulative distribution for signal and noise information
for i = 1:1:length(x)
cum_sum_Signal(i)=sum(percent_sum_Signal(1,i:length(percent_sum_Signal)));
cum_sum_Noise(i)=sum(percent_sum_Noise(1,i:length(percent_sum_Signal)));
end
```

7.4 Code to calculate the optimal value to distinguish signal information from noise information

The code below is continuing of the previous code. We kept the name of variables of the previous code in the follow code.

```
x = min_Noise:interval:max_Signal; %Interval including SNR of Noise and Signal information
FA = cum_sum_Noise; %False positive rate
HIT = cum_sum_Signal; %True positive rate
m = length(FA);
trade_off = ones(1,m);
%Next loop will calculate of the trade-off in the ROC space
for i = 1:m
   trade_off(1,i) = abs(FA(1,i)-HIT(1,i));
end
counter = 1;
maximum_trade_off = max(trade_off);%Finding the maximum trade-off between hit and false alarm
```

```
%Next loop will find the position of the maximum_trade_off in the matrix trade_off
for i = 1:m
   if (maximum_trade_off == trade_off(1,t))
      break
   else
      counter = counter + 1;
   end
end
Optimal_SNR = x(1,counter);%Optimal_SNR is the SNR value in the same position in x of maximum_trade_off in trade_off.
```

8. Conclusion

The multifocal electroretinogram is a relatively new method of visual investigation and studies that contribute to the improvement of the effectiveness of the method should be encouraged. The method described in this chapter intended to assist in the neuroophthalmological diagnosis by estimating ranges of SNR as indicators of the quality of the electrophysiological response.

9. Acknowledgements

Supported by FINEP research grant "Rede Instituto Brasileiro de Neurociência (IBN-Net)" #01.06.0842-00, CNPq-PRONEX / FAPESPA #2268, CNPq #486351/2006-8, CNPq #550671/2007-2, CNPq #620037/2008-3, CNPq #476744/2009-1, CNPQ #475860/2010-1. ACC received a CNPq fellowship for graduate students. DFV and LCLS are CNPq research fellows.

10. References

Greenstein, V.C., Holopigian, K., Seiple, W., Carr, RE., & Hood, D.C. (2004). Atypical multifocal ERG responses in patients with diseases affecting the photoreceptors. *Vision Research*, Vol. 44, No. 25, (November 2004), pp. 2867-2874, ISSN 0042-6989

Hood, D.C., Holopigian, K., Greenstein, V., Seiple, W., Li, J., Sutter, E.E., & Carr, R.E. (1998). Assessment of local retinal function in patients with retinitis pigmentosa using the multi-focal ERG technique. *Vision Research*, Vol. 38, No. 1, (January 1998), pp. 163-179, ISSN 0042-6989

Hood, D.C., Odel, J.G., Chen, C.S., & Winn, B.J. (2003). The multifocal electroretinogram. *Journal of Neuro-Ophthalmology*, Vol. 23, No. 3, (September 2003), pp. 225-235, ISSN 1536-5166

Hood, D.C., Bach, M., Brigell, M., Keating, D., Kondo, M., Lyons, J.S. & Palmowski-Wolfe, A.M. (2008). ISCEV guidelines for clinical multifocal electroretinography (2007 edition). *Documenta Ophthalmologica*, Vol. 116, No. 1, (January 2008), pp. 1-11, ISSN 0012-4486

Huang, H.J., Yamazaki, H., Kawabata, H., Ninomiya, T., & Adachi-Usami, E. (1997). Multifocal electroretinogram in multiple evanescent white dot syndrome. *Documenta Ophthalmologica*, Vol. 92, No. 4, (December 1996), pp. 301-309, ISSN 0012-4486

Kretschmann, U., Seeliger, M.W., Ruether, K., Usui, T., Apfelstedt-Sylla, E., & Zrenner, E. (1998). Multifocal electroretinography in patients with Stargardt's macular dystrophy. *British Journal of Ophthalmology*, Vol. 82, No. 3, (March 1998), pp. 267-275, ISSN 0007-1161

Raster, M., Horn, F., Jüneman, A., Rosa, A.A., Souza, G.S., Gomes, B.D., Lima, M.G., Silveira, L.C., & Kremers, J. (2011). Retinal disorders in northern Brazilian patients treated with chloroquine assessed by multifocal ERG. *Documenta Ophthalmologica*, Vol. 122, No. 2, (April 2011), pp. 77:86, ISSN 0012-4486

Seeliger, M.W., Kretschmann, U.H., Apfelstedt-Sylla, E., & Zrenner, E. (1998). Implicit time topography of multifocal electroretinograms. *Investigative Ophthalmology and Visual Science*, Vol. 39, No. 5, (April 1998), pp. 718-723, ISSN

Sutter, E.E., & Tran, D. (1992). The field topography of ERG components in man – I. The photopic luminance response. *Vision Research*, Vol. 32, No. 3, (March 1992), pp. 433-446, ISSN 0042-6989

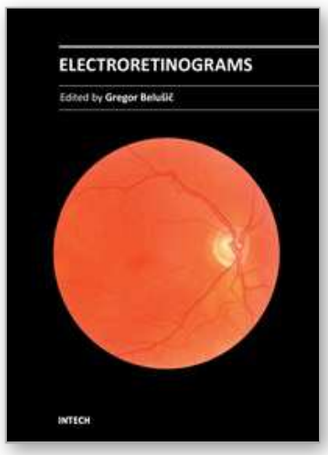
Sutter, E.E. (2000). The interpretation of multifocal binary kernels. *Documenta Ophthalmologica*, Vol. 100, No. 2-3, (March 2000), pp. 49-75, ISSN 0012-4486

Sutter, E.E. (2001). Imaging visual function with the multifocal m-sequence technique. Vision Research, Vol. 41, No. 10-11, (May 2001), pp. 1241-1255, ISSN 0042-6989

Ventura, D.F., Costa, M.F., Berezowsky, A., Salomão, S.R., Simões, A.L., Lago, M., Pereira, L.H., Faria, M.A., De Souza, J.M., & Silveira, L.C. (2004). Multifocal and full-field electroretinogram changes associated with color-vision loss in mercury vapor exposure. *Visual Neuroscience*, Vol. 21, No. 3, (May 2004), pp. 421-9, ISSN 0952-5238

Wright, T., Nilsson, J., Gerth, C., & Westall, C. (2008). A comparison of signal detection techniques in the multifocal electroretinogram. *Documenta Ophthalmologica*, Vol. 117, No. 2, (September 2008), pp. 163-170, ISSN 0012-4486

Zhang X, Hood DC, Chen CS, Hong JE (2002). A signal-to-noise analysis of multifocal VEP responses: an objective definition for poor records. *Documenta Ophthalmologica*, Vol. 104, No. 3, (May 2002), pp. 287-302, ISSN 0012-448



Electroretinograms

Edited by Dr. Gregor Belusic

ISBN 978-953-307-383-5

Hard cover, 238 pages

Publisher InTech

Published online 09, August, 2011

Published in print edition August, 2011

Electroretinography (ERG) is a non-invasive electrophysiological method which provides objective information about the function of the retina. Advanced ERG allows to assay the different types of retinal receptors and neurons in human and animal models. This book presents contributions on the recent state of the ERG. The book is divided into three parts. The first, methodological part, reviews standard methods and normatives of human ERG, reports about the advanced spatial, temporal and spectral methods of stimulation in human ERG, and deals with the analysis of the multifocal ERG signal. The second part deals with the ERG in different diseases of the human visual system and in diabetes. The third part presents the ERG in the standard animal models of human retinal disease: mouse, rat, macaque and fruitfly.

How to reference

In order to correctly reference this scholarly work, feel free to copy and paste the following:

Aline Corrêa de Carvalho, Givago da Silva Souza, Bruno Duarte Gomes, Anderson Raiol Rodrigues, Dora Fix Ventura and Luiz Carlos de Lima Silveira (2011). Method to Indentify Nonsignificant Responses at Multifocal Electroretinogram Recordings: Technical Note, Electroretinograms, Dr. Gregor Belusic (Ed.), ISBN: 978-953-307-383-5, InTech, Available from: http://www.intechopen.com/books/electroretinograms/method-to-indentify-nonsignificant-responses-at-multifocal-electroretinogram-recordings-technical-no

INTECH

open science | open minds

InTech Europe

University Campus STeP Ri
Slavka Krautzeka 83/A
51000 Rijeka, Croatia
Phone: +385 (51) 770 447
Fax: +385 (51) 686 166
www.intechopen.com

InTech China

Unit 405, Office Block, Hotel Equatorial Shanghai
No.65, Yan An Road (West), Shanghai, 200040, China
中国上海市延安西路65号上海国际贵都大饭店办公楼405单元
Phone: +86-21-62489820
Fax: +86-21-62489821

© 2011 The Author(s). Licensee IntechOpen. This chapter is distributed under the terms of the Creative Commons Attribution-NonCommercial-ShareAlike-3.0 License, which permits use, distribution and reproduction for non-commercial purposes, provided the original is properly cited and derivative works building on this content are distributed under the same license.

IntechOpen

IntechOpen